U.S. DEPARTMENT OF THE INTERIOR
U.S. GEOLOGICAL SURVEY

Statistical Property of the Earth Reflectivity and Fractal Seismic Deconvolution

by
Myung W. Lee[1]

Open-File Report 95-697

1U.S. Geological Survey, Box 25046, Denver Federal Center, Denver, CO 80225

Table of Contents

Figures

Tables

ABSTRACT

The observed reflection seismogram is the convolution of a source wavelet with the earth reflectivity function and the primary purpose of deconvolution is to remove the effect of wavelet on the seismogram. Conventionally, wavelet deconvolution is accomplished under the assumptions that earth reflectivity is a white sequence and the phase of the source wavelet is minimum. However, the earth reflectivities computed from well logs suggest that the power spectra are proportional to the power of the frequency (a power law), and autocorrelation functions show significant negative values at lags 1 and 2, which implies nonwhiteness.

Incorporating the observed behavior of the earth reflectivities using 2 or 3 terms of autocorrelation function significantly improves the performance of deconvolution over a conventional spiking deconvolution when the reflection coefficients series is assumed to be earth reflectivity function(or impulse response). However, including random noise and inner-bed multiples degrades the performance of deconvolution.

Because the statistics of the earth reflectivity is not known in most cases, a practical way of incorporating the negative autocorrelation at small lags is applying a two-term shaping filter $(1+\gamma Z)$ with reasonable filter coefficients (γ) between -0.1 and -0.6.

INTRODUCTION

Observed seismograms reveal complex interferences due to the effects of source wavelets and consequently the original data provide low resolution of sedimentary sequences. The essence of seismic deconvolution is to remove the wavelet effect from the original data and improve the resolution of reflected events. Much research has been done in the areas of seismic deconvolution (Wadsworth and others, 1953; Robinson, 1957; Peacock and Treitel, 1969). If the source wavelet is known, deterministic approaches can be attempted. However, because the input wavelet is not known in most cases, statistical methods are commonly applied. In the statistical approach, a deconvolution operator is designed by making assumptions about the statistics of reflection sequence.

The most common assumption of statistical deconvolution is that the earth reflectivity is a white sequence and the phase of the source wavelet is minimum. Under these assumptions, a spiking deconvolution is equivalent to a wavelet deconvolution (Robinson, 1957; Peacock and Treitel, 1969). When the phase of the wavelet is not minimum, there remains some residual phase error in the deconvolved output, but the output is a white sequence.

Walden and Hosken (1985) demonstrated that reflection coefficients from a wide variety of rock sequences around world are nonwhite. They showed that the reflection sequences are pseudo-white only above a corner frequency, below which their power spectrum falls away according to a power law ω^{α}, where α is between 0.5 and 1.5. This spectrum can be adequately modeled by an ARMA(1,1) process (Autoregressive-moving average with a single pole and a single zero). When the exponent is 1, the autocorrelation function decays very rapidly and only 2 terms of the autocorrelation are enough to describe the statistics of the reflectivity (Todoeschuck and Jensen, 1989).

In order to incorporate the pseudo-whiteness of the earth reflectivity, Walden and Hosken (1985) proposed a new seismic deconvolution method by deriving an ARMA shaping filter. They assumed that the earth reflectivity can be decomposed into the convolution of the ARMA(1,1) shaping filter and the white noise sequence. The property of nonwhiteness of the reflection coefficients is also utilized in the design of the deconvolution operator using an autocorrelation of the reflectivity sequence (Todoeschuck and Jensen, 1988; Todoeschuck and Jensen, 1989; Todoeschuck, 1994). Todoeschuck and Jensen (1989) showed that a simple modification to the prediction error filter or spiking filter significantly improves the

deconvolution for nonwhite reflection sequences and provided an example showing that the error between the known reflection sequences and that recovered by the conventional spiking filter was 20 %, but it was 0.5 % using the new approach, about 40 fold improvement in reducing the error. However, Todoeschuck (1994) indicated that this new approach did not work well with the real data because the peg-leg multiples or inner-bed multiples alter the statistical property of the reflectivity.

In this paper, in addition to deriving a deconvolution filter by solving nonlinear normal equations using autocorrelations up to lag = 2, a much simpler shaping filter approach is presented.

ACKNOWLEDGEMENTS

I would like to thank John J. Miller and Warren F. Agena for their helpful comments.

THEORY

Seismic traces can be approximated by the following convolutional model denoting * as a convolution operator in the time domain:

$$s(t) = h\{r(t)\} * w(t) + n(t) \tag{1}$$

where

$s(t)$ = seismic trace,

$h\{r(t)\}$ = earth reflectivity or impulse response,

$r(t)$ = reflection coefficient,

$w(t)$ = source wavelet, and

$n(t)$ = noise.

The objective of seismic deconvolution is to remove the wavelet effect from the seismic trace and recover the earth reflectivity function. Let's define a filter function f(t) in such a way that if the filter is applied to the observed seismic trace, the output is the estimation of earth reflection coefficient or earth reflectivity function. In other words,

$$e(t) = s(t) * f(t) \tag{2}$$

where $e(t)$ is the estimated earth reflectivity.

The computation of the inverse filter f(t) is easily accomplished, if the source wavelet is known. When the source wavelet is not known, a statistical estimation method under some assumptions can be applied. The well known spiking deconvolution filter is based on the assumption that the earth reflectivity is a white sequence. Because the earth reflectivity is a white sequence, the autocorrelation function is zero except at zero lag.

Let's derive a more general deconvolution filter based on the nonwhiteness of the earth reflectivity function.

A) Time Domain Solution Using Normal Equation

The autocorrelation function of the estimated earth reflectivity is given by:

$$A_n = \sum_k e_k e_{n-k}$$

$$= \sum_k \sum_m f_m s_{k-m} \sum_l f_l s_{n-k-l}$$

$$= \sum_m f_m \sum_l f_l Q_{m+n-l} \qquad (3).$$

In equation (3), Q is the autocorrelation of the observed seismogram and is different from the autocorrelation of the estimated earth reflectivity function because of the wavelet effect. Let's minimize the zero-lag autocorrelation function (A_0) with respect to the filter coefficient in Equation (3), as in Todoeschuck and Jensen (1989). The resulting equation is:

$$\sum_n f_n Q_{i-n} = 0. \qquad (4)$$

If Equation (4) is satisfied when i> 0, it cab be shown that $A_n = 0$ for n greater than 0. Thus Equation (3) with Equation (4) can be written by the following matrix equation.

$$\begin{pmatrix} Q_0 & Q_1 & \cdots & \cdots & Q_K \\ Q_1 & Q_0 & Q_1 & \cdots & Q_{K-1} \\ . & . & . & . & . \\ . & . & . & . & . \\ Q_K & Q_{K-1} & \cdots & .. & Q_0 \end{pmatrix} \begin{pmatrix} f_o \\ f_1 \\ . \\ . \\ f_K \end{pmatrix} = \begin{pmatrix} A_0 \\ 0 \\ . \\ . \\ 0 \end{pmatrix}. \qquad (5)$$

Equation (5) is the same as that used in the design of a spiking deconvolution filter (Peacock and Treitel, 1969). As indicated in Equation (5), the autocorrelation of the output using this deconvolution filter (a spiking deconvolution filter) is zero except at the zero lag.

If an assumption is made that Equation (4) is satisfied for i > 1, then it is shown that $A_i = 0$ for i > 1. In general, it can be shown that by making $A_i = 0$ for i > I in Equation (4), the autocorrelation function of the reflectivity in Equation (3) is non-zero up to I-th lag. Therefore Equation (3) with the condition of Equation (4) provides a general deconvolution filter for the specified autocorrelation function of the earth reflectivity. If the autocorrelation function is non-zero up to lag 2, the following matrix equation can be easily derived:

$$\begin{pmatrix} Q_0 & Q_1 & \cdots & \cdots & Q_K \\ Q_1 & Q_0 & Q_1 & \cdots & Q_{K-1} \\ . & . & . & . & . \\ . & . & . & . & . \\ Q_K & Q_{K-1} & \cdots & .. & Q_0 \end{pmatrix} \begin{pmatrix} f_o \\ f_1 \\ . \\ . \\ f_K \end{pmatrix} = \begin{pmatrix} A_0 - f_1 (A_1 - f_2 A_2) \\ A_1 - f_1 A_2 \\ A_2 \\ . \\ 0 \end{pmatrix} \qquad (6)$$

This is a nonlinear equation for the filter coefficients f and can be solved by an iterative method.

When the earth reflectivity is assumed to be white, the magnitude of A_0 in Equation (5) is immaterial, so Equation (5) can be solved based on the observed seismic traces. However, in general, the relative values of the autocorrelation function for given lags greater than 0 must be known in solving Equation (6). So Equation (6) can not be solved based on the observed seismogram without some knowledge of the statistical behavior of the reflectivity. Todoeschuck (1994) labeled this new approach of deconvolution fractal deconvolution.

B) Frequency Domain Solution Using Spectral Decomposition

The above derivation of a deconvolution operator for nonwhite reflectivity can be formulated in the context of a shaping filter in the frequency domain. Let's assume that Fourier transformed variables are denoted as capital letters (e.g. $S(\omega)$ is the Fourier transform of s(t)), then Equation (1) can be written as follows under the assumption that the earth reflectivity function is the same as the reflection coefficient series (primary impulse response):

$$S(\omega) = R(\omega)W(\omega) + N(\omega). \tag{7}$$

If we define a filter $F(\omega)$ as an inverse operator of wavelet, that is

$$F(\omega) = \frac{W^*(\omega)}{W(\omega)W^*(\omega) + \sigma} \approx \frac{1}{W}(\omega). \tag{8}$$

In Equation (8), the asterisk denotes a complex conjugate and σ is a constant.

Let's assume that the phase of the wavelet is minimum and the autocorrelation of the wavelet, not the wavelet itself, is known. Then a wavelet can be derived by a spectral decomposition of the wavelet autocorrelation function (Claerbout, 1976; Robinson and Treitel, 1980). Because a wavelet can be estimated, an inverse operator can be derived as shown in Equation (8). The autocorrelation of the observed seismogram $\Phi(\omega)$ without noise can be written as follows the frequency domain:

$$\begin{aligned} \Phi(\omega) &= S(\omega)S^*(\omega) \\ &= R(\omega)R^*(\omega)W(\omega)W^*(\omega) \\ &= \Phi_-(\omega)\Phi_+(\omega)W(\omega)W^*(\omega) \qquad (9a) \\ &= cW(\omega)W^*(\omega), \qquad (9b) \end{aligned}$$

where Φ_+ and Φ_- are the spectral decomposition of the autocorrelation function $\Phi(\omega)$ and c is a constant.

Equation (9b) is true when the reflectivity sequence is white. In this case, the wavelet autocorrelation function is a scaled version of the autocorrelation function of the seismogram and a wavelet inverse filter (let's denote it as F_s) can be derived from the observed seismogram with a minimum phase assumption. Therefore, the output of the filter derived in Equation (5) and F_s provide the same autocorrelation function, and the autocorrelation function of the output is

$$S(\omega)S^*(\omega)F_s(\omega)F_s^*(\omega) \approx R(\omega)R^*(\omega) = c. \tag{10}$$

Notice that Equation (10) is valid when the reflectivity is assumed to be white and the filter (F_s) is derived using only the zero-lag autocorrelation function of the observed seismogram (a spiking deconvolution operator). Let's multiply the spectral decomposition of autocorrelation function, Equation (9a), to both sides of Equation (10).

$$\begin{aligned} \Phi_+(\omega)\Phi_-(\omega)S(\omega)S^*(\omega)F_s(\omega)F_s^*(\omega) &= c\Phi_+(\omega)\Phi_-(\omega) \\ S(\omega)F(\omega)S^*(\omega)F^*(\omega) &= c\Phi_+(\omega)\Phi_-(\omega). \qquad (11) \end{aligned}$$

If we define $F(\omega) = \Phi_+(\omega)F_s(\omega)$as as in Equation (11), then the output autocorrelation function deconvolved with $F(\omega)$ is the scaled version of the autocorrelation function of the earth reflectivity. Therefore the filter $\Phi_+(\omega)F_s(\omega)$ is equivalent to the filter derived from Equation (4). In other words,$\Phi_+(\omega)F_s(\omega)$ shapes the output autocorrelation function into the desired

autocorrelation function, instead of the function itself.

The shaping filter approach presented here is similar to the one proposed by Walden and Hosken (1985). They proposed to use an ARMA (1,1) (A polynomial with a single pole and a single zero) shaping filter. Here a moving average type shaping filter based on the spectral decomposition of the autocorrelation function is presented. Both approaches are fundamentally equivalent in that they try to shape the output autocorrelation into a desired form.

The implementation of Equation (11) can be easily demonstrated by the following example. Let's assume that the autocorrelation function can be written in the following form, using the Z-transform, assuming that only two values (lag 0 and lag 1) are non-zero.

$$A(Z) = \frac{A_1}{Z} + A_0 + A_1 Z,$$

$$= \beta(Z+\gamma)\left(\frac{1}{Z}+\gamma\right),$$

$$= \Phi_- \Phi_+. \tag{12}$$

In the Z-transform, Φ_- is the solution of spectral decomposition whose zeroes are inside a unit circle and Φ_+ is the solution whose zeroes are outside a unit circle. The spectral decomposition of the autocorrelation function can be accomplished by finding γ in Equation (12). The solution is given with $A_0 = 1$,

$$\gamma = \frac{1-\sqrt{1-4A_1^2}}{2A_1}. \tag{13}$$

Similarly, the three term autocorrelation function can be decomposed by finding roots of the cubic equation.

Because the output of the spiking deconvolution is white, the order of application of Equation (11) is important. The proper sequence is:

1) Firstly, derive a spiking deconvolution operator using the observed seismogram and apply it to the data.

2) Secondly, perform spectral decomposition of the autocorrelation function of earth reflectivity and apply this minimum phase function to the deconvolved output.

In this paper, the minimum phase function computed from the first two terms of autocorrelation function is called a two-term shaping filter and a three-term shaping filter when the first 3 terms of autocorrelation function are used for the filter design.

CHARACTERISTICS OF EARTH REFLECTIVITY

As mentioned in the previous section, when the earth reflectivity is a white sequence, a spiking deconvolution is equivalent to a wavelet deconvolution under the assumption of a minimum phase source wavelet. When the reflectivity sequence is white, the power spectrum of the time series is a uniform function of the frequency. How accurate is this white sequence of the earth reflectivity ? In order to examine the behavior of the power spectrum of earth reflectivity with respect to the frequency, reflection coefficient series were analyzed. The reflection coefficient series was computed from sonic logs with 1 ms sampling interval (two-way time). Figures 1-2 show examples of amplitude spectra of the reflection coefficient series at 4 different wells. A power spectrum of a time series is given by the Fourier transform of the corresponding autocorrelation function.

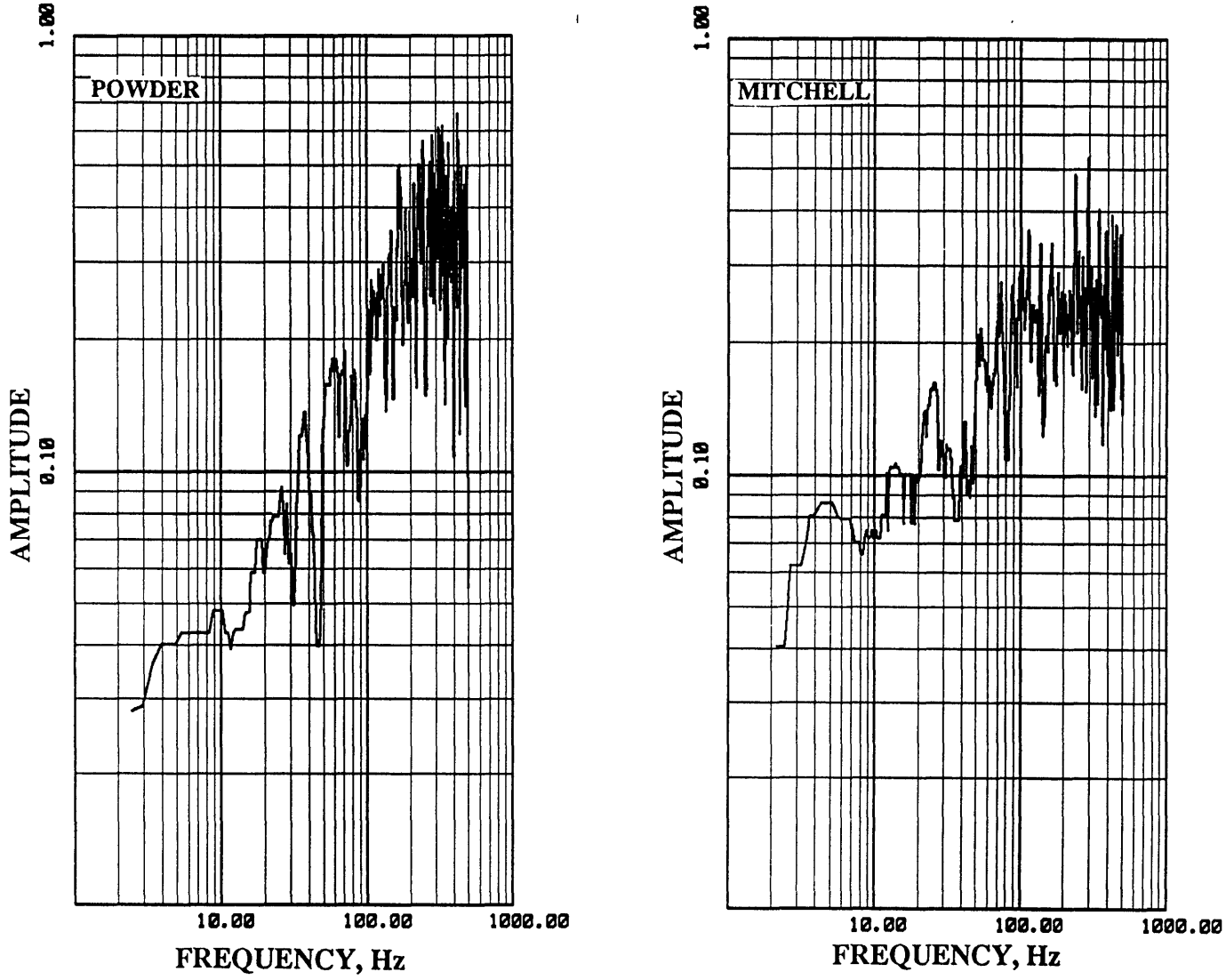

Figure 1. Amplitude spectra for the reflection coefficient series at the Powder and Mitchell wells.

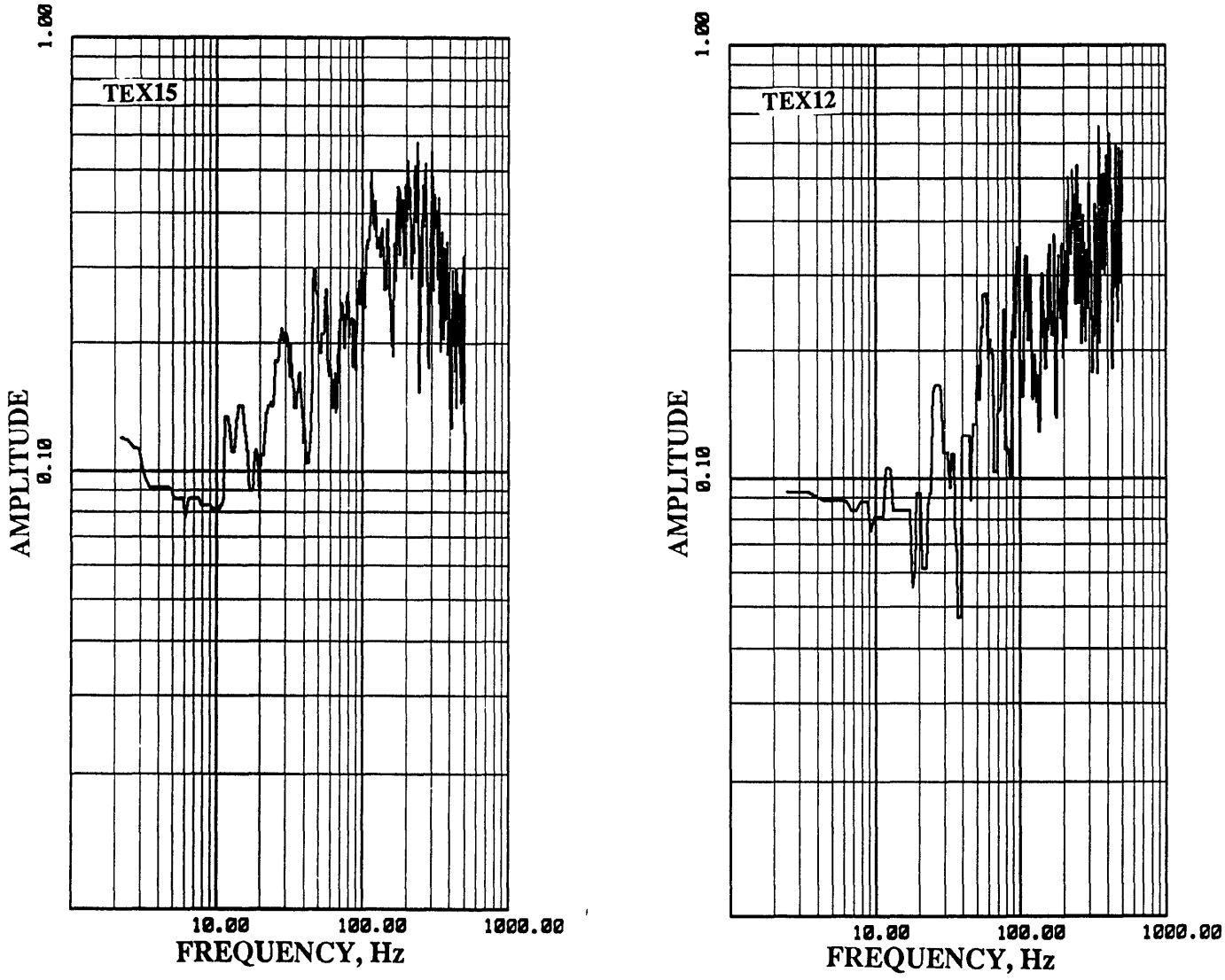

Figure 2. Amplitude spectra for the reflection coefficient series at the Tex15 and Tex12 wells.

All the amplitude spectra of reflection series indicate diminishing of the low frequency content relative to high frequency content. Let's assume that the power spectrum of the reflectivity function is proportional to the some power α of the frequency (ω):

$$P \approx \omega^{\alpha}.$$

This is one class of random fractals known as the Gaussian scaling noises (Mandelbrot, 1982). A sample of a Gaussian scaling noise has a Gaussian probability distribution. Because the Gaussian scaling noise is a power function of frequency, a log-log plot of frequency versus power shows a linear trend. The examples shown in Figures 1 and 2 indicate this linear trend to varying degrees. The slopes of the least squares fit to the power spectra, parameter α, shown in Figures 1 and 2 are 1.05, 0.47, 0.39, 0.87 for the Powder, Mitchell, Tex15 and Tex12 wells respectively. If the reflection series is a white sequence, the slope of the power spectra should be close to 0 or flat in the log-log plot. Therefore, it is shown that the reflection coefficient series shown in Figures 1 and 2 are not white sequences.

The autocorrelation functions of reflection coefficients for the time lag up to 5 msec are shown in Table I. The autocorrelation values at lag 1 and lag 2 indicate large negative values except for the Tex15 well. Negative values at small lags are characteristic of the autocorrelation function of reflection sequences generated from well logs (O'Doherty and Anstey ,1971).

Lag, ms	Powder	Mitchell	Tex12	Tex15	Powder*	Tex15*
0	1.0	1.0	1.0	1.0	1.0	1.0
1	-0.308	-0.14	-0.36	0.03	-0.131	0.04
2	-0.184	-0.145	-0.08	-0.33	-0.07	-0.12
3	0.01	-0.04	0.01	-0.10	0.00	0.01
4	-0.01	-0.02	-0.06	0.01	0.00	0.05

Table I, The normalized autocorrelation functions of reflection coefficient series for lags up to 4 ms. Superscript * indicates the seismic response including all inner-bed multiples except the surface multiple.

The reflection coefficient series is an approximation of earth reflectivity function, because the earth reflectivity should include all multiples, particularly short-period inner-beds multiples. The amplitude spectra of earth reflectivity functions including all inner-bed multiples except a free-surface multiple are shown in Figure 3 for the Powder and Tex15 wells. Notice the relative increase of low-frequency content compared to the amplitude spectra of the reflection coefficients. The least squares estimations of slope parameter α are 0.237 and 0.02 for the Powder and Tex15 wells respectively, and are much close to the expected parameters for a white sequence.

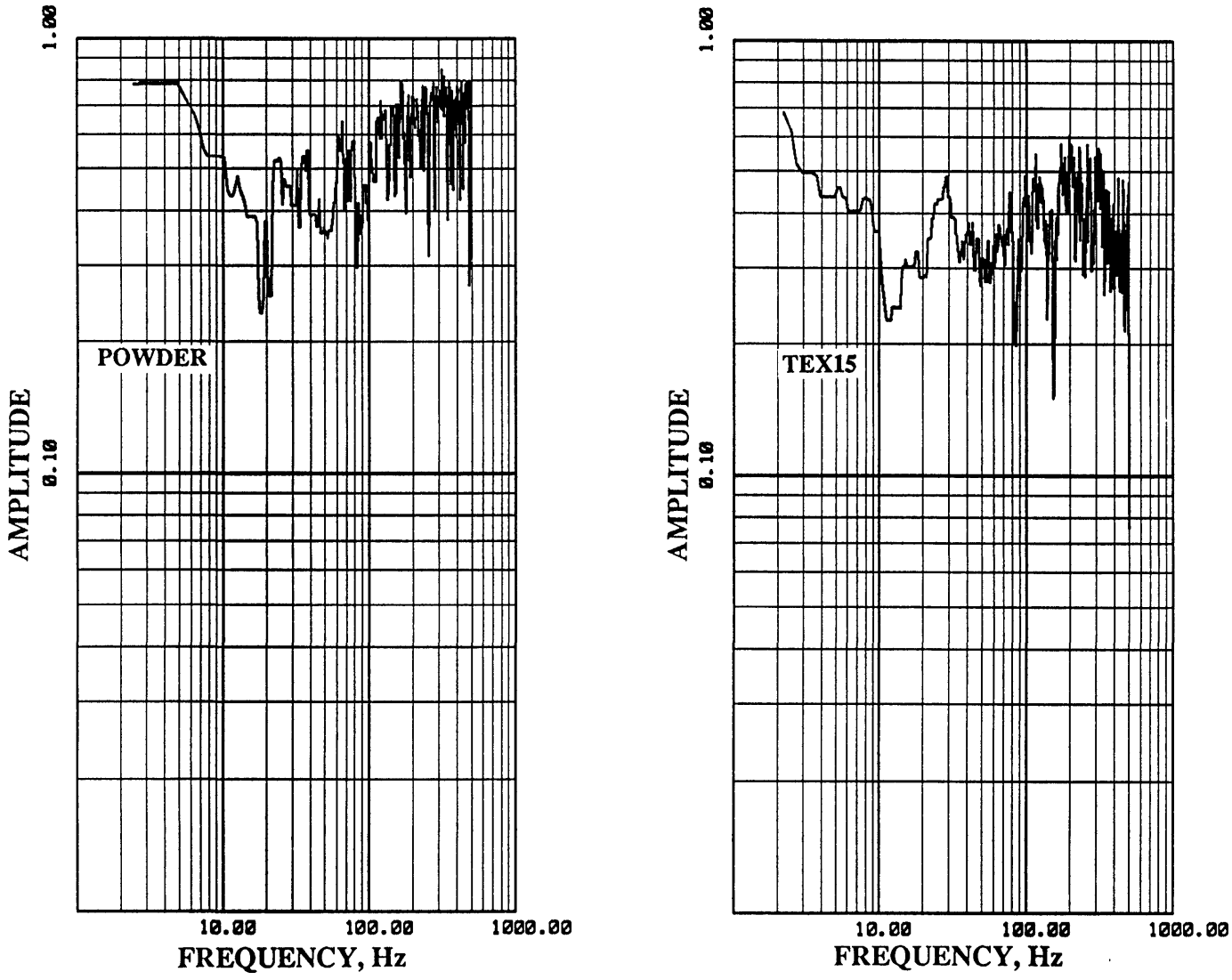

Figure 3. Amplitude spectra for the impulse response including inner-bed multiples at the Powder and Tex15 wells.

NUMERICAL EXAMPLES

A)Primary Response Without Noise

In order to investigate the effect of the autocorrelation function on the performance of deconvolution operator, the reflection coefficient series used to generate the spectrum in Figure 1, the Powder well, was used. Figure 4 shows deconvolved outputs with various assumptions about the autocorrelation function. The phase of input wavelet is a minimum phase with a peak frequency of 100 Hz and it is given by

$$w(t) = e^{-0.15} \sin(\pi t/5).$$

Figure 4A represents the reflection coefficient series, which is assumed to be the earth reflectivity. The convolution of reflection coefficients with the minimum phase wavelet (input for the deconvolution example) is shown in Figure 4B. Shown in Figure 4C is the error sequence of the output after an 11 point spiking deconvolution operator is applied to input data. Figure 4D represents the error sequence of output when a deconvolution operator using Equation (6) under the assumption that the autocorrelation function has only two values (lag 0 and lag 1) and all other values are zero is applied, and Figure 4E shows the result of applying Equation (6) under the assumption that the autocorrelation has three non-zero values (lag 0, lag 1 and lag 2) and all other autocorrelation values are zero. An error sequence is defined as the difference between the true earth reflectivity function and estimated reflectivity function through the deconvolution. The root-mean-square error, which is defined as the RMS value of the error sequence divided by the RMS value of input, of the results shown in Figure 4 are 54 %, 22 % and 9 % for Figure 4C, 4D and 4E respectively. The output of Figure 4E and RMS values indicates that the deconvolution with the assumption of three non-zero autocorrelation function is almost perfect, while the output of the spiking deconvolution shows the large error in the output. Using 3 term autocorrelation improves the performance of deconvolution by about 3 times that of using 2 term autocorrelation. As indicated in Table I, the autocorrelation function of the reflection coefficient at the Powder Well shows significant non-zero values at lag 1 and lag 2. Equation (6) tries to honor the input autocorrelation as accurately as possible and the result proves that the formula shown in Equation (6) adequately handles the statistical property of the reflection series.

The input for the spiking deconvolution is the seismogram itself (i.e., Figure 4B). However the input for the Figures 4D and 4E requires the normalized autocorrelation function of the true reflection coefficients, which is not generally available. The autocorrelation function of the deconvolved output for Figure 4D indicates that the normalized autocorrelation function at lag 1 is -0.424 instead of the input -0.308 (Table II). The discrepancy of the autocorrelation function result from the way the nonlinear equation is solved. In the computer program, the optimum filter coefficients f_0 and f_1 of Equation (6) are computed to get the minimum RMS error values for the output. As we can see later, this does not happen when a shaping filter approach is used. The autocorrelation of the deconvolved output for Figure 4E is $1.0 - 0.303Z - 0.187Z^2$. This is very similar to the input autocorrelation function, because there are no significant autocorrelation values after lag 2.

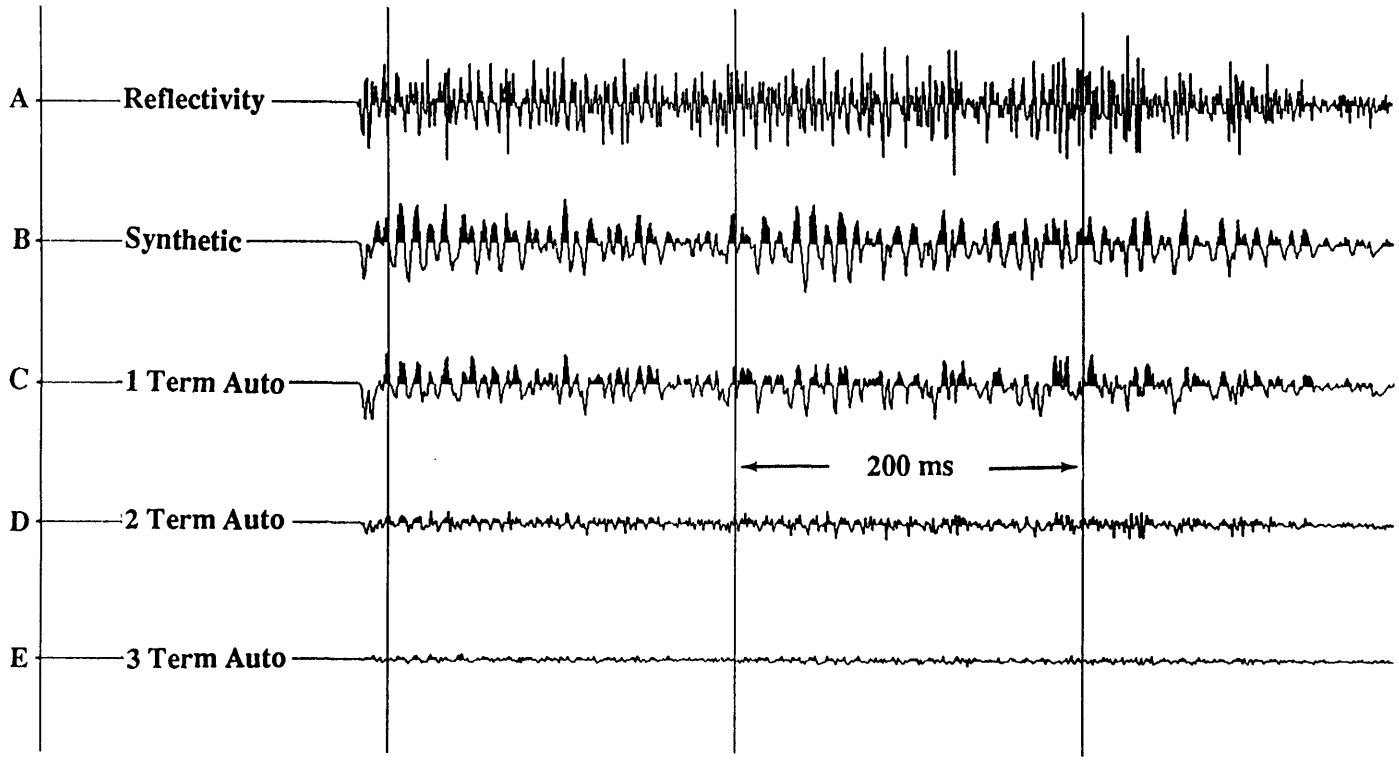

Figure 4. Deconvolved outputs without random noise using a nonlinear normal equation. An 11 point long fractal deconvolution operator was derived from Figure 4B incorporating the autocorrelation function shown in Table I. A) Reflection coefficient series at the Powder well. B) Wavelet convolved seismogram. C) The error sequence for the spiking deconvolution. D) The error sequence for the fractal deconvolution using a 2 term autocorrelation. E) The error sequence for the fractal deconvolution using a 3 term autocorrelation.

Lag, ms	Figure 4A	Figure 4B	*Figure 4C	*Figure 4D	*Figure 4E	*Figure 5D	*Figure 5E
0	1.000	1.000	1.000	1.000	1.000	1.000	1.000
1	-0.308	0.638	-0.003	-0.424	-0.303	-0.308	-0.304
2	-0.184	0.055	-0.008	-0.004	-0.187	-0.003	-0.182
3	0.007	-0.387	-0.016	-0.003	-0.001	-0.008	-0.003
4	-0.010	-0.557	-0.017	0.001	0.003	-0.005	0.001

Table II. The autocorrelation functions for the input and deconvolved outputs shown in Figures 4 and 5. Superscript * indicates that the actual input is not the error function shown in Figures 4 and 5, but the actual deconvolved output.

The deconvolved output using the shaping filter approach is shown in Figure 5 using same format as for Figure 4. The RMS error values are 58 %, 28 % and 10% for Figures 5C, 5D, and 5E respectively. The autocorrelation function of the deconvolved output is shown in Table II. As indicated in Table II, the autocorrelation function of output matches the input autocorrelation function quite well. However, the RMS values of error indicate that the performance based on the shaping filter approach is apparently somewhat inferior to the output when using Equation (6). It must be emphasized that there would have been no performance difference between the two approaches, if the actual input has only two non-zero autocorrelation values for Figure 4D and Figure 5D or only three non-zero autocorrelation values for Figure 4E and Figure 5E.

B) Intrabed Multiple and Noise Effect

The effect of the random uncorrelated Gaussian noise on the performance of deconvolution is shown in Figure 6 for the signal to noise ratio (S/N) of 5 and in Figure 7 for the S/N of 2. The RMS errors between true and deconvolved outputs are 54 %, 32 %, and 23 % for Figures 6C, 6D, and 6E respectively. Improvement of about 2 fold in the RMS error has been achieved by honoring the 3 term autocorrelation function. However the RMS errors are 62 %, 50% and 48% for Figures 7C, 7D, and 7E respectively. In this case, the improvement by using a 2 or 3 term autocorrelation function of reflection series is marginal.

As mentioned before, the reflection coefficient series is an approximation of the earth impulse response. The results for the earth impulse response including all the inner-bed multiples except the surface multiple is shown in Figure 8 using the format as that of Figure 5. The RMS errors between the true earth reflectivity and the deconvolved output are 17 %, 9%, and 6% for Figures 8C, 8D, and 8E respectively. This example indicates that the effect of autocorrelation function at small lags on the deconvolution when including inner-bed multiples is less significant than that of the primary only case (Figure 5).

DISCUSSION

A) Earth Reflectivity

Spectral analyses indicate that the reflection coefficient sequence is better approximated by a power law in the frequency domain than by a white spectrum and the analyses from 4 wells indicate that the exponent for the power law varies between 0.4 and 1.0. Walden and Hosken (1985) reported that the exponent varies between 0.5 and 1.5 by analyzing 8 wells from a wide

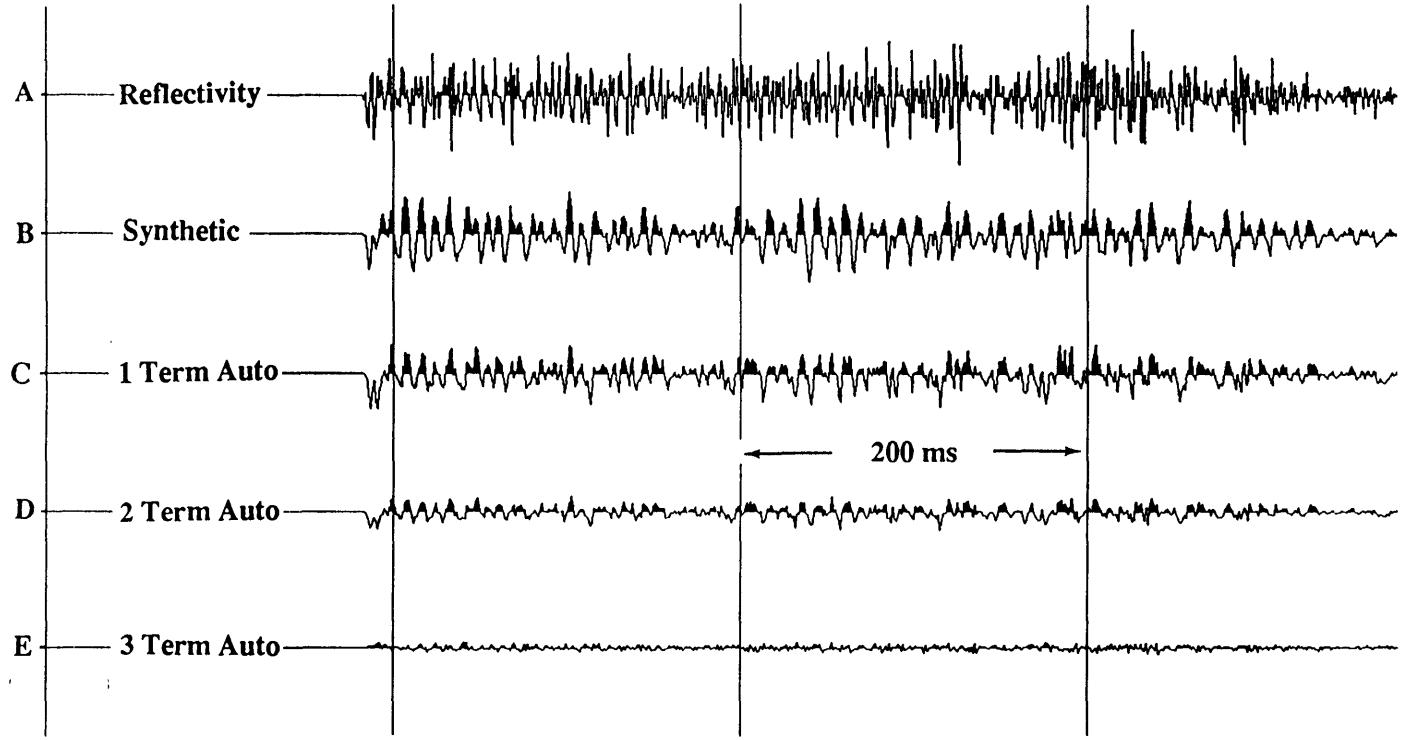

Figure 5. Deconvolved outputs without random noise using the shaping filter approach. An 11 point long spiking filter was derived from Figure 5B. A) Reflection coefficient series at the Powder well. B) Wavelet convolved seismogram. C) The error sequence for the spiking deconvolution. D) The error sequence for the fractal deconvolution using a 2 term shaping filter. E) The error sequence for the fractal deconvolution using a 3 term shaping filter.

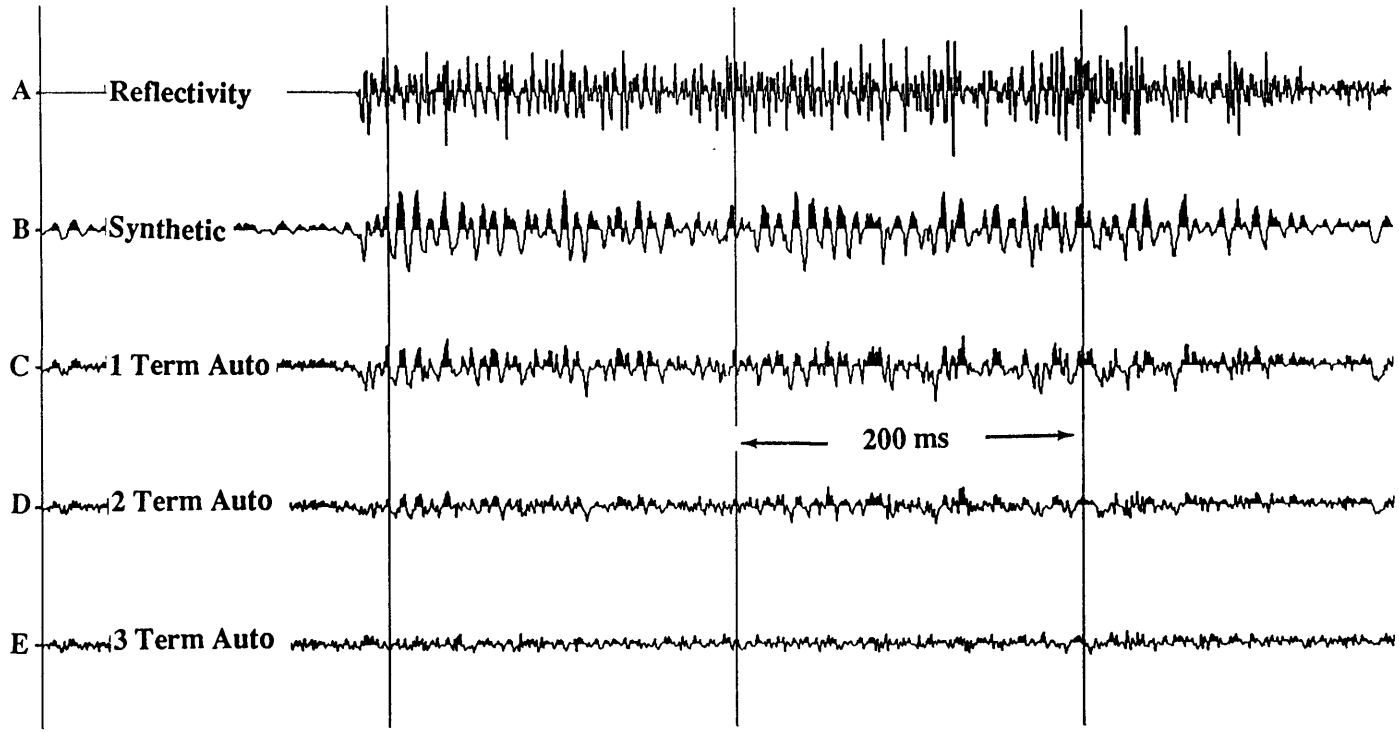

Figure 6. Deconvolved outputs using the shaping filter approach for the reflection series at Powder well with random noise (S/N of 5). An 11 point long spiking filter was derived from Figure 6B. A) Reflection coefficient series. B) Wavelet convolved seismogram. C) The error sequence for the spiking deconvolution. D) The error sequence for the fractal deconvolution using a 2 term shaping filter. E) The error sequence for the fractal deconvolution using a 3 term shaping filter.

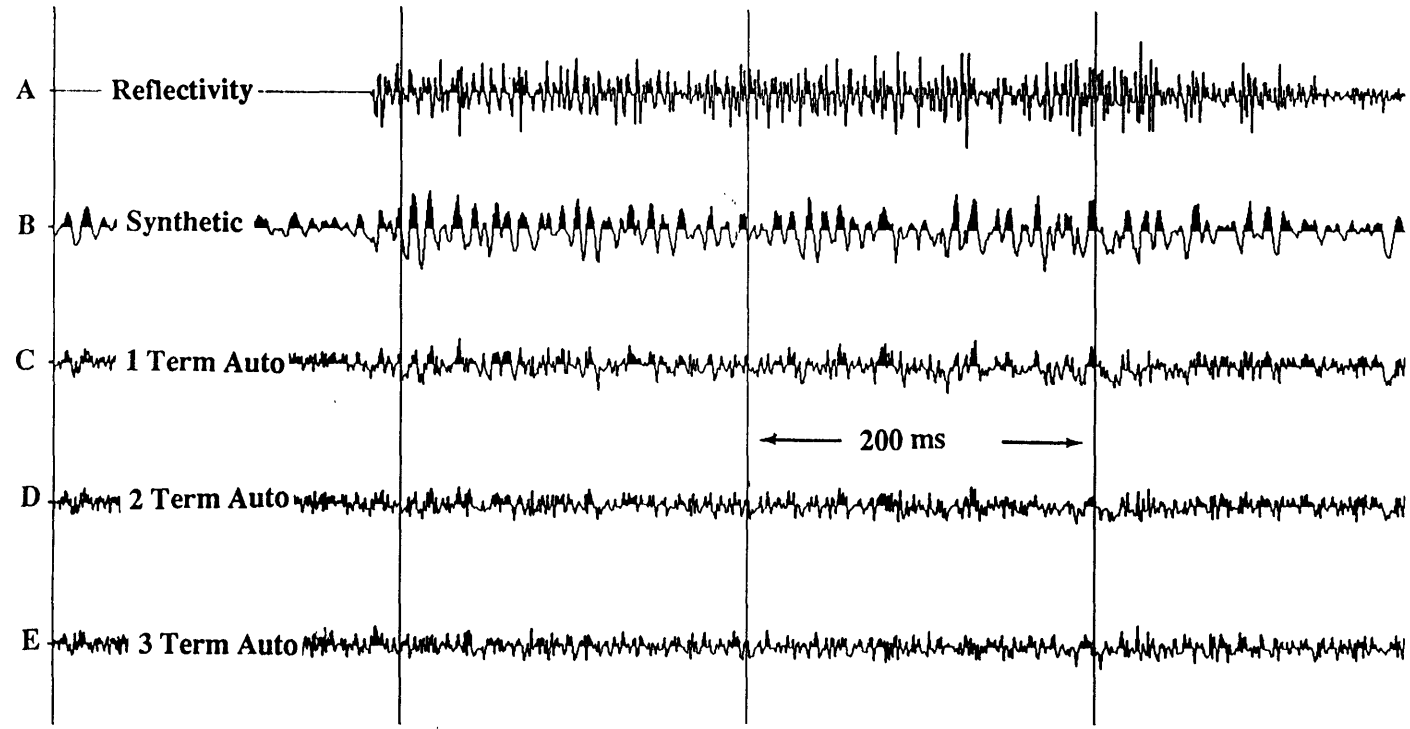

Figure 7. Deconvolved outputs using the shaping filter approach for the reflection series at Powder well with random noise (S/N of 2). An 11 point long spiking filter was derived from Figure 7B. A) Reflection coefficient series. B) Wavelet convolved seismogram. C) The error sequence for the spiking deconvolution. D) The error sequence for the fractal deconvolution using a 2 term shaping filter. E) The error sequence for the fractal deconvolution using a 3 term shaping filter.

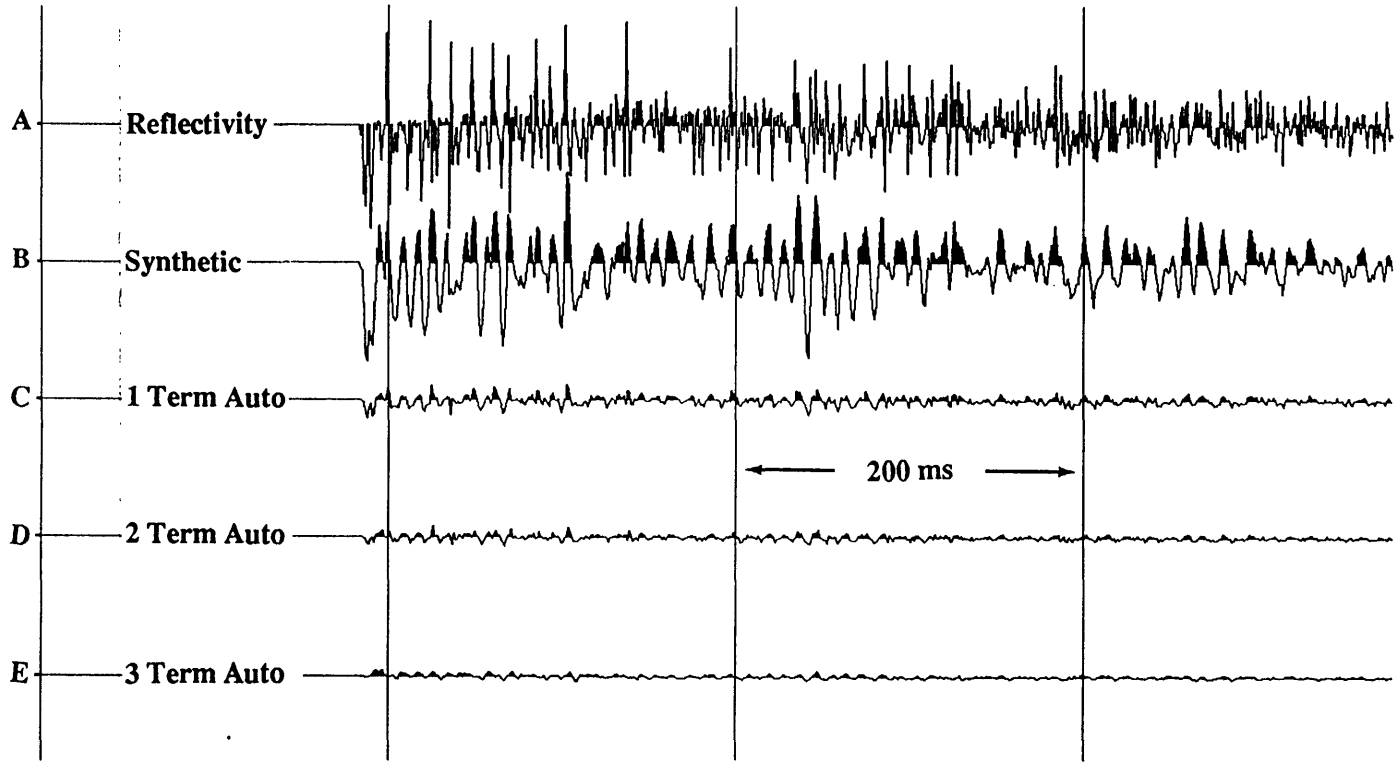

Figure 8. Deconvolved outputs using the shaping filter approach for the impulse response including inner-bed multiples reflection series at the Powder well without random noise. An 11 point long spiking filter was derived form Figure 8B. A) Reflection coefficient series. B) Wavelet convolved seismogram. C) The error sequence for the spiking deconvolution. D) The error sequence for the fractal deconvolution using a 2 term shaping filter. E) The error sequence for the fractal deconvolution using a 3 term shaping filter.

variety of geographical locations and geological sequences. The positive value of the exponent implies the low-cut behavior of reflection coefficient series and is a manifestation of negative autocorrelations at small lags (Walden and Hosken, 1985).

If the reflection sequence is white, the autocorrelation values can be ignored except at lag 0. However, Table I indicates that the autocorrelations of reflection sequences contain significant contributions at correlation lags greater than 0. Theses large negative autocorrelations at small lag and the low-cut behavior of the reflection sequence (Figure 1) confirms Walden and Hosken (1985). Table I also indicates that the autocorrelation of the reflection coefficient can be approximated by the first 3 terms. These negative autocorrelations at small lags have significant implications for the design of deconvolution operator.

B) Fractal Deconvolution

The conventional spiking deconvolution assumes that the earth reflectivity sequence is white and the autocorrelation of the reflectivity is zero except at zero lag. Numerical examples indicate that significant improvement in the performance of the deconvolution operator can be achieved by including more autocorrelation values of the earth reflectivity (Figures 4 and 5). However, the improvements of the fractal deconvolution over conventional spiking deconvolution degrades as inner-bed multiples are included and the noise content increases (Figures 6, 7 and 8).

The effect of inner-bed multiples and random noise on the autocorrelation function is to increase the value of zero-lag autocorrelation. Schoenberge and Levin (1974) demonstrated that the intrabed (inner-bed) multiples tend to raise the amplitudes at the low-frequency end of the spectrum and lower those at the high-frequency end (apparent attenuation). This low-pass filtering effect is evident in Figure 3. The low pass filtering effect of the intrabed multiples manifested itself by reducing the relative strength of the negative values of autocorrelation at small lags. The A_1 and A_2 of the reflection coefficients are -0.308 and -0.184 respectively, but those values including intrabed multiples are reduced to -0.131 and -0.07 (Table I), a reduction of about 3 fold. Also, adding uncorrelated random noise to the seismogram only increases the value of the zero-lag autocorrelation. Thus the effect of autocorrelation values at small lags in the design of the fractal deconvolution operator is reduced when intrabed multiples or random noises are included. For example, the improvement in the RMS error of deconvolved output by an operator including 3 term autocorrelation function for Powder well over the spiking deconvolution is about 6 fold when reflection sequences is used for earth impulse responses, but it is only about 3 fold when inner-beds multiples are included. Also note that the RMS error for Figure 5E (deconvolution using 3 term autocorrelation function) is almost identical to that for Figure 8C (spiking deconvolution).

Numerical examples suggest that the iterative method, solution of Equatuion (6), in deriving a deconvolution operator using Equation (6) seems to work better than the shaping filter approach (Compare Figure 4 and Figure 5). However, these two approaches are essentially the same. The apparent discrepancy between the two approaches is due to fact that the iterative method keys on minimizing the error in the output rather than preserving the input autocorrelation as accurate as possible. The output autocorrelation value at lag = 1 for Figure 4D is -0.424, which differs from the input autocorrelation value of - 0.308. Whereas the autocorelation value at lag 1 for Figure 5D is -0.308, which is identical to the input autocorelation value. However, the RMS error for Figure 4D is much smaller than that for Figure 5D. This implies that the fratcal deconvolution filter derived from the PEF method somewhat compensated the effect of autocorelation at lag 2 by altering the output autocorreltion value at lag = 1. When this output autocorrelation value is used for the 2-term shaping filter

approach, the RMS of the error function is $1.3X10^{-2}$, which is the same RMS value for the error function computed from applying Equation (6). This analysis concludes that the underlying principle for two approaches for the fractal deconvolution is the same.

C) Practical Considerations

As indicated in the previous examples, the effectiveness of a three-term shaping filter over a two-term shaping filter decreases as random noise and inner-bed multiples are increased. Also, because the autocorrelation function of earth reflectivity is not known in most cases, designing a two-term shaping filter is more practical than designing a three-term shaping filter when processing real data. Equation (13) indicates that the theoretical minimum value of negative autocorrelation at lag = 1 is -0.5. Table I shows that the negative autocorrelation value at lag = 1 ranges from -0.14 to -0.308 except at the Tex15 well. A practical approach may be to design two-term shaping filters with various A_1 in the range of -0.1 to -0.5 and examine the output. Because true reflectivity is not known except in the case of where well logs are available, the user should decide logically which filter performs best. Figure 9 shows this approach. Various two-term filters were computed using A_1 between -0.1 and -0.5 and applied to the spiking deconvolved trace (Figure 9C). The RMS values for the error function are 54 %, 46 %, 37 %, 29 %, 23 %, and 35 % for Figure 9C, 9D, 9E, 9F, 9G and 9H respectively. In this case we know that the minimum error occurs near $A_1 = -0.4$, but in real data processing we cannot determine which value is best for the data set without any other knowledge.

The general form of the shaping filter is $1+\gamma Z$, where γ is between 0 and -1.0. Filter coefficients are -0.1, -0.21, -0.33, -0.5, -0.63, and -1.0, for A_1 = -0.1, -0.2, -0.3, -0.4, -0.45, and -0.5 respectively. When $A_1 = -0.5$, $\gamma = -1.0$. In this case the two-term shaping filter is a differential operator. Figure 10 shows the amplitude spectra of these various two-term filters with respect to γ when the temporal sample rate is 1 ms. For values of $\gamma > -0.5$, the shaping filter does almost nothing when frequencies are less than about 100 Hz. This suggests that the advantage of the fractal deconvolution in processing conventional surface seismic data, where frequency content is usually less than 80 Hz, is insignificant and conventional spiking deconvolution works well.

CONCLUSIONS

This paper showed how to incorporate autocorrelation function up to small lags in the design of deconvolution operator and provided synthetic examples. This study concludes that:
1) The autocorrelations of reflection coefficients show non-negligible negative values at small lags and the spectral behavior implies the nonwhiteness of the sequence. The power spectra of the reflection coefficients for the 4 wells studied here approximately varies with ω^{α}, where α is between 0.4 and 1.0. The autocorrelation function of the earth reflectivity can be approximated by the first 3 terms.
2) Applying a shaping filter derived from the spectral decomposition of the autocorrelation function after the spiking deconvolution is equivalent to applying a deconvolution operator derived from the solution of a nonlinear normal equation. The shaping filter approach offers remarkably simple computational implementation.
3) Significant improvements of deconvolution using 2 or 3 terms of the autocorrelation function can be achieved when the reflection coefficients are used for the earth impulse response. However, the performance degrades as random noises and inner-bed multiples are included in the seismogram. This implies that the improvement of this new deconvolution method over the conventional spiking deconvolution is marginal when processing real data.

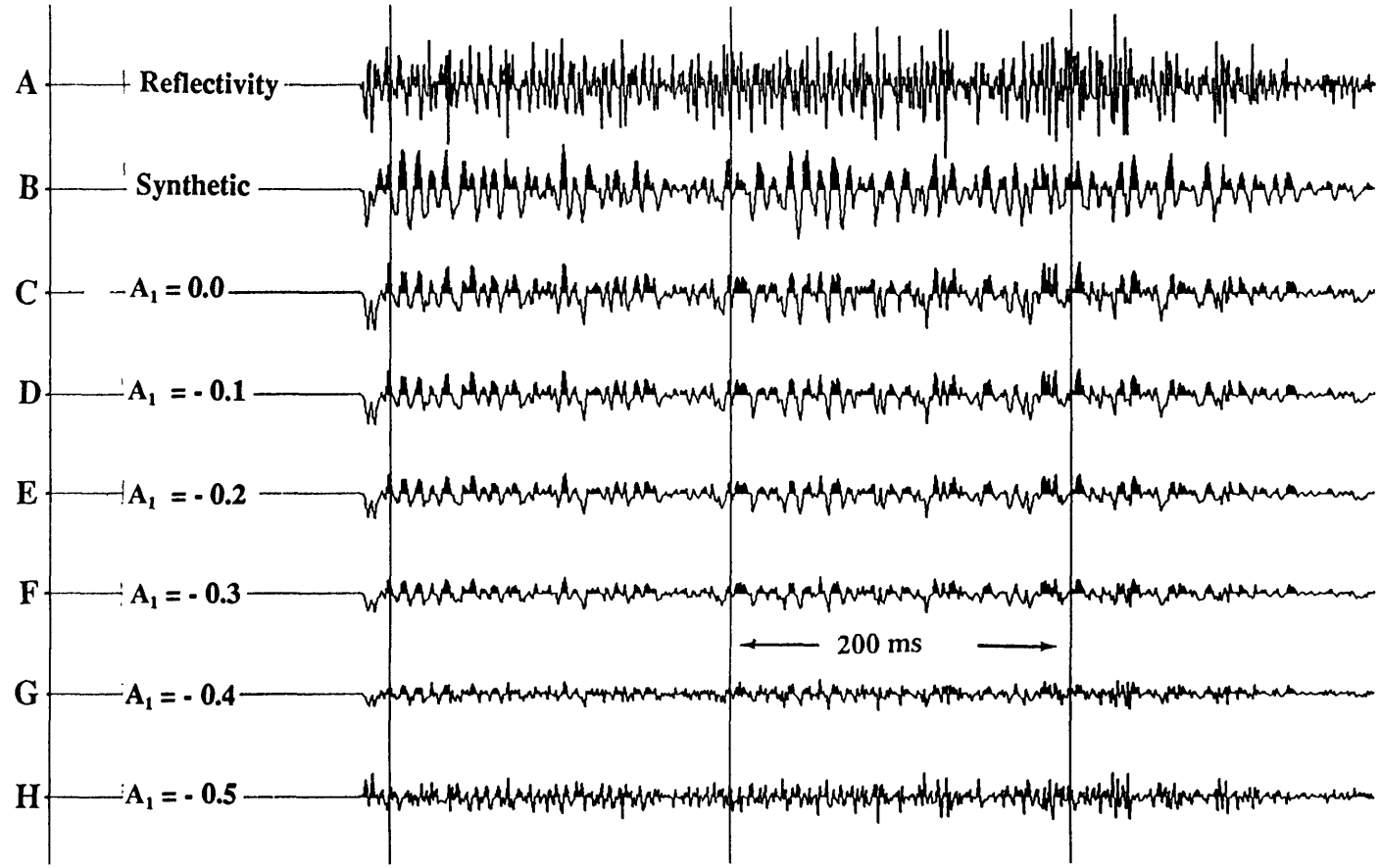

Figure 9. Graph showing the effect of the various autocorrelation values at lag = 1 (A_1) on the fractal deconvolution using the two term shaping filter approach. An 11 point long spiking filter was derived from Figure 9B. A) Reflection coefficient series at the Powder well. B) Wavelet convolved seismogram. C) The error sequence for the spiking deconvolution (A_1 = 0.0). D, E, F, G, H) The error sequence for the fractal deconvolution with A_1 = -0.1, A_1 = -0.2, A_1 = -0.3, A_1 = -0.4, and A_1 = -0.5 respectively.

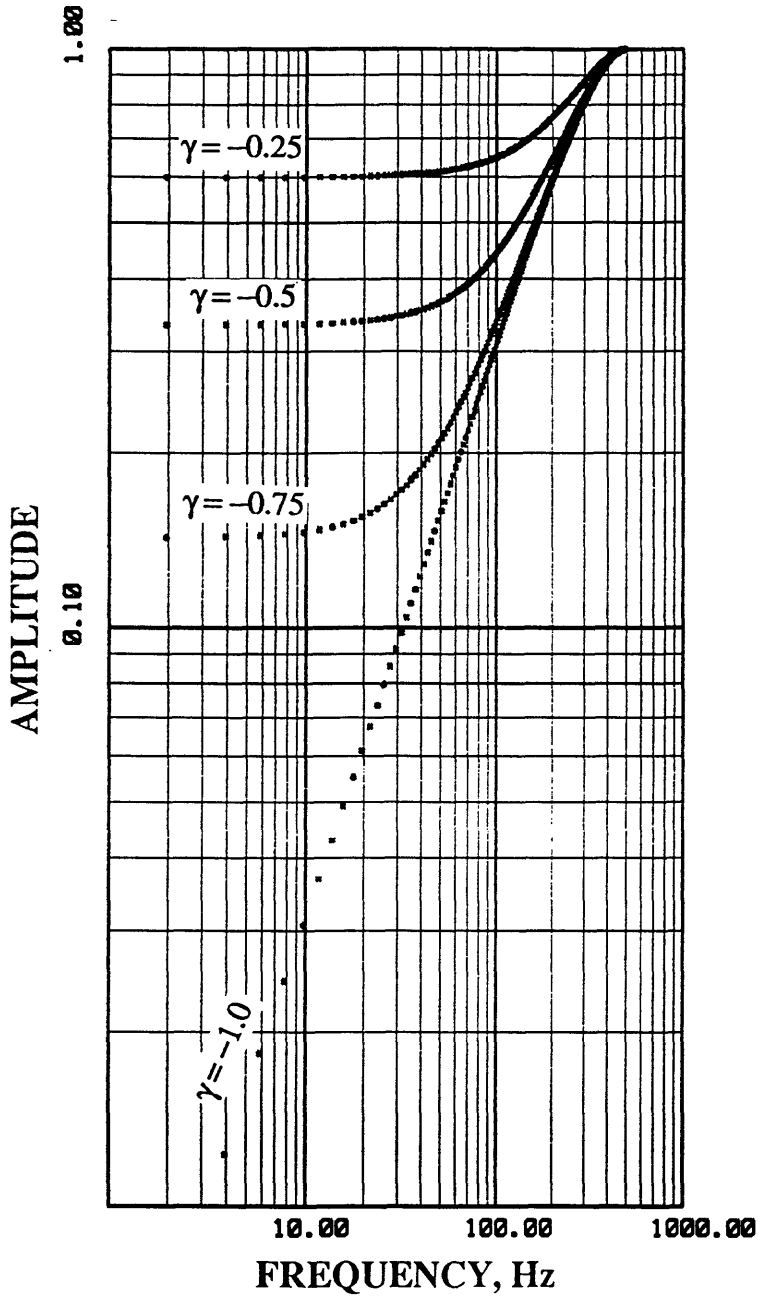

Figure 10. Fourier amplitude spectra for the 2-term shaping filters in the form of $F(Z) = 1.0 + \gamma Z$, where γ is between -0.25 to -1.0. Sampling interval is 1 ms.

4) In real data processing, a simple 2-term shaping filter in the form of $1+\gamma Z$, where γ is between -0.1 and -0.6 can be applied to the data after spiking deconvolution. This shaping filter can be considered as a post-deconvolution spectral shaping filter. The reasonable choice of γ depends upon the interpretability of the processed section.
5) When the frequency content is less than about 80 Hz, conventional spiking deconvolution is adequate.

REFERENCES

Claerbout, J.F., 1976, Fundamentals of geophysical data processing: With applications to petroleum prospecting: MaGraw-Hill Book Co., New York, 274 p.

Mandelbrot, B.B., 1982, The fractal geometry of nature: W.H. Freeman & Co., San Francisco, 460 p.

O'Doherty, R.F. and Anstey, N.A., 1971, Reflections on amplitudes: Geophysical Prospecting, v. 19, p. 430-458.

Peacock, K.L. and Treitel Sven, 1969, Predictive deconvolution: Theory and practice: Geophysics, vol. 34, p. 155-169.

Robinson, E.A., 1957, Predictive decomposition of seismic traces: Geophysics, vol. 22, p. 767-778.

Robinson, E.A. and Treitel, S., 1980, Geophysical signal analysis: Prentice-Hall, Inc., Englewood Cliffs, 466 p.

Schoenberger, M. and Levin, F.K., 1974, Apparent attenuation: Geophysics, v. 39, p. 278-291.

Todoeschuck, J.P., 1994, Fractal deconvolution revisited, Expanded abstracts: SEG International Exposition and 64th Annual Meeting Oct. 23-29, Los Angeles, p. 739-742.

Todoeschuck, J.P. and Jensen, O.G.,1988, Joseph geology and seismic deconvolution: Geophysics, vol 53, p. 1410-1414.

Todoeschuck, J.P. and Jensen, O.G.,1989, Scaling geology and seismic deconvolution: Pure and applied Geophysics, vol 131, p. 273-287.

Wadsworth, G.P., Robinson, E.A., Bryan, J.G., and Hurley, P.M., 1953, Detection of reflections on seismic records by linear operations: Geophysics, vol, 18, p. 539-586.

Walden, A.T. and Hosken, J.W.J., 1985, An investigation of the spectral properties of primary reflection coefficients: Geophysical prospecting, vol. 33, p. 400-435.